

Nuclear Bragg Scattering of Synchrotron Radiation with Strong Speedup of Coherent Decay, Measured on Antiferromagnetic $^{57}\text{FeBO}_3$

U. van Bürck and R. L. Mössbauer

Physik-Department E15, Technische Universität München, D-8046 Garching, Federal Republic of Germany

E. Gerdau, R. Ruffer, and R. Hollatz

II. Institut für Experimentalphysik, Universität Hamburg, D-2000 Hamburg 50, Federal Republic of Germany

G. V. Smirnov

I. V. Kurchatov Institute of Atomic Energy, Moscow, U.S.S.R.

and

J. P. Hannon

Physics Department, Rice University, Houston, Texas 77001

(Received 22 April 1987)

A strongly speeded-up decay of a collective nuclear excitation has been observed in pure nuclear resonance diffraction of synchrotron-radiation pulses by a perfect single crystal of antiferromagnetic $^{57}\text{FeBO}_3$. Superimposed appeared a quantum-beat spectrum exhibiting the interference of four hyperfine transitions. The angular dependence of the time spectrum was verified with measurements above, below, and at the exact Bragg position. The off-Bragg measurements reveal sensitively the weak quadrupole interaction in $^{57}\text{FeBO}_3$.

PACS numbers: 75.50.Gg, 07.85.+n, 42.10.Qj, 76.80.+y

Pulsed synchrotron radiation allows measurements of the time structure of the decays of nuclear excited states. Radiative decays can be observed in pure nuclear reflections from single crystals, which appear in selected Bragg directions. If a perfect single crystal containing resonant nuclei is excited at the Bragg position, decay modes appear which because of their coherent nature proceed much faster than in individual nuclei.^{1,2} If the nuclear levels are split by hyperfine fields, there is an additional quantum-beat modulation of the coherent decay rate.³⁻⁵

We report on measurements of the pure nuclear Bragg reflection from a perfect single crystal of $^{57}\text{FeBO}_3$. The measurements give a striking demonstration of the speedup of coherent decay and show a quantum-beat pattern, corresponding to the response characteristic for any simple ^{57}Fe antiferromagnet. There is a pronounced asymmetry in the amplitudes of the quantum beats above and below the Bragg angle, which gives a direct measure of the weak quadrupole shifts of the hyperfine lines.

Pure nuclear resonant diffraction by single crystals of $^{57}\text{FeBO}_3$ has been studied for many years with conventional ^{57}Co sources.^{6,7} The compound is nearly antiferromagnetic at room temperature, with a slightly canted spin system lying in the $\{111\}$ planes. The electric field gradient (EFG) is perpendicular to these planes. The $\{hhh\}$ reflections with odd h are suppressed for the non-resonant electronic x-ray scattering but allowed for the resonant scattering by the nuclei. With improved growth techniques,⁸ nearly perfect crystals of FeBO_3 enriched to

95% in ^{57}Fe are available with sizes up to $1 \times 1 \text{ cm}^2$.

The experimental arrangement was the same as in a previous experiment,⁵ but now with ^{57}Fe -YIG (yttrium iron garnet) replaced by $^{57}\text{FeBO}_3$. Following a Si premonochromator and a Ag mirror, the beam incident on the $^{57}\text{FeBO}_3$ crystal had a divergence of $\sigma \approx 10 \mu\text{rad}$. Measurements were made with the beam centered at, $\approx 30 \mu\text{rad}$ above, and $\approx 20 \mu\text{rad}$ below the Bragg angle for the pure nuclear reflection (111). The crystal of about 1 cm^2 , allowing a beam cross section of $1 \times 10 \text{ mm}^2$, was placed in a weak external magnetic field perpendicular to the scattering plane ($\mathbf{k}_0, \mathbf{k}_f$) in order to align the internal fields parallel to $\mathbf{k}_0 + \mathbf{k}_f$. The resonant diffraction spectrum then consists of four well separated lines arising from the four " $\Delta J_z = \pm 1$ " transitions (J_z is not precise for crossed B and EFG). The relative positions of the resonance energies are shown in Fig. 1. The results of the measurements and the theoretical calculations are given in Fig. 2.

A striking feature of the time response shown in Fig. 2 is the dramatic speedup of the coherent decay. In Figs. 2(a)–2(c), the top dotted lines correspond to the exponential decay characteristic of an individual nucleus, with lifetime $\hbar/\Gamma = 141 \text{ ns}$, while the dashed lines tangent to the envelopes of the initial observed response give initial lifetimes $\tau \approx 17 \text{ ns}$ at the Bragg angle, and $\approx 24 \text{ ns}$ above and below the Bragg angle, corresponding to a speedup by factors of ≈ 8 and ≈ 6 with respect to the natural lifetime \hbar/Γ (≈ 68 and ≈ 45 with respect to the lifetime \hbar/Γ_γ for pure γ decay). A fourfold speedup of the decay rate was also present in the measure-

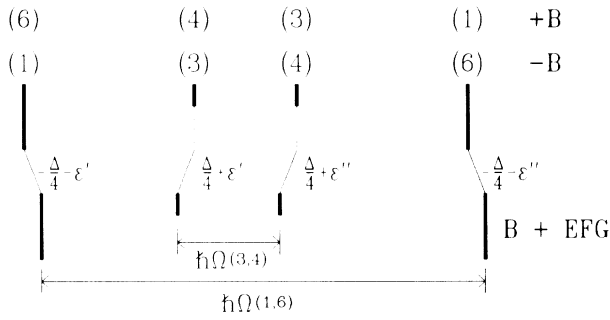


FIG. 1. Hyperfine splittings between the four “ $\Delta J_z = \pm 1$ ” transitions in iron borate. Here the transitions are (1) $= [+\frac{1}{2} \leftrightarrow +\frac{3}{2}]$, (3) $= [+\frac{1}{2} \leftrightarrow -\frac{1}{2}]$, (4) $= [-\frac{1}{2} \leftrightarrow +\frac{1}{2}]$, and (6) $= [-\frac{1}{2} \leftrightarrow -\frac{3}{2}]$. In the drawing the ϵ shifts of the full Hamiltonian are added. The room-temperature values are $\hbar\Omega(1,6) \approx \hbar\Omega_M(1,6) = 110.5\Gamma$, $\hbar\Omega(3,4) \approx \hbar\Omega_M(3,4) = 17.5\Gamma$, $\Delta = -3.9\Gamma$, $\epsilon' = +0.06\Gamma$, $\epsilon'' = -0.06\Gamma$ with $\Gamma = 4.665 \times 10^{-9}$ eV.

ments on $^{57}\text{Fe-YIG}$,^{4,5} but there it is largely masked by the slow quantum-beat modulation. (A previous observation⁹ of a speedup in $^{57}\text{Fe}_2\text{O}_3$ is rather questionable because of poor statistics.) Measurements of the speedup using radioactive sources were recently carried out with a nanosecond magnetic shutter,¹⁰ whereas the corresponding broadening of the width has been observed in the frequency studies of the $^{57}\text{FeBO}_3$ reflection.⁶

The exact nature of the speedup of coherent decay varies, depending on the scattering system. For $^{57}\text{FeBO}_3$ at room temperature, the hyperfine splitting is so strong that there are four well separated resonances. In this case the response is essentially that of an isolated resonance modulated by the fast quantum-beat spectrum from the four oscillators. For a thick-crystal Bragg reflection¹¹ or grazing-incidence reflection¹² of synchrotron-radiation pulses, the response of a well isolated resonance is

$$|R(t, \Theta)|^2 \propto \exp\{-[\Gamma/\hbar + 2\omega_B''(\Theta)]t\} |J_1(\omega_B(\Theta)t)|^2/t^2, \quad (1)$$

where ω_B is the complex dynamical beat frequency. For the (111) Bragg reflection in $^{57}\text{FeBO}_3$, ω_B of the strongest “ $\Delta J_z = \pm 1$ ” transition is given by $\omega_B(\Theta) = \omega_B' - i\omega_B'' = (63\Gamma/\hbar)(0.93\delta\Theta + i)^{-1}$ where $\delta\Theta = \Theta - \Theta_{\text{Bragg}}$ is the rocking angle about Bragg in microradians. For the initial response the decay is dominated by the leading factor, giving a nearly exponential initial decay at the rate $\Gamma/\hbar + 2\omega_B''(\Theta)$. At the Bragg angle, this exponential decay is strongly enhanced (by a factor of 127), but the approximation is only valid up to $t \approx 2$ ns. Off the Bragg angle, the initial exponential decay is only very weakly enhanced, but the decay becomes considerably speeded up at later times $t > |\omega_B(\Theta)|^{-1}$. This behav-

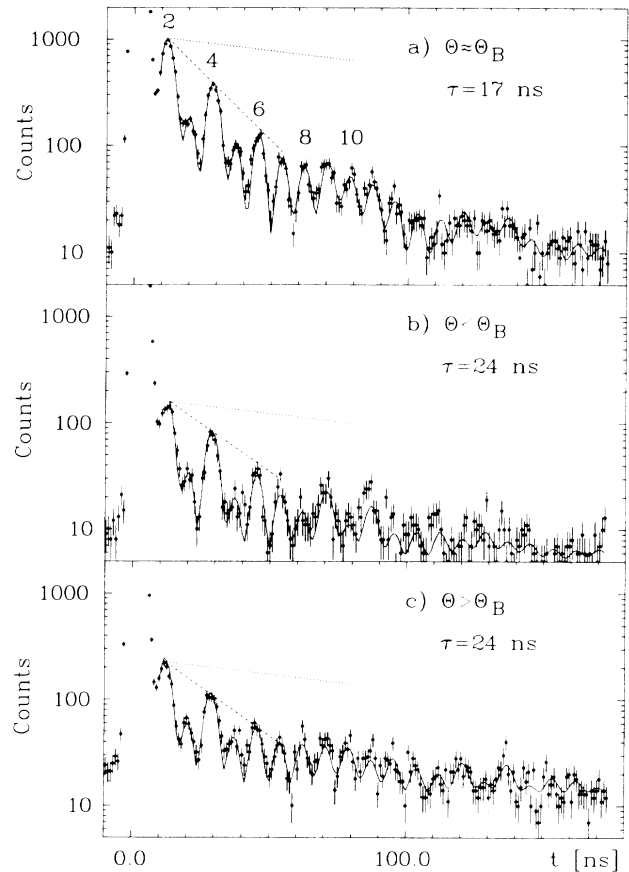


FIG. 2. Time spectra of the coherently scattered radiation measured at different angular positions: (a) exact Bragg angle, (b) $\approx 20 \mu\text{rad}$ below Bragg angle, and (c) $\approx 30 \mu\text{rad}$ above Bragg angle. The solid lines are the calculated theoretical spectra averaged over a Gaussian spread of $30 \mu\text{rad}$ plus a constant background contribution. The dotted lines show a natural exponential decay $\exp(-\Gamma/\hbar t)$, and the dashed lines show the initial enhanced decay with lifetime τ . The ratio of delayed to prompt counts is about 1×10^{-3} . All data were accumulated within a day.

ior of the time spectrum^{11,12} is due to dynamical beats, which are the result of the non-Lorentzian response of the resonance. Thus the speeded-up decay given by Eq. (1) is strongly angle and time dependent. For the actual experimental conditions the time dependence has to be computed from the dynamical theory.¹⁻³

Almost all features of the quantum-beat spectrum can be understood in the Born approximation. The splitting of the four contributing transitions is shown in Fig. 1, with the corresponding relative strengths of the transitions being $+1$, $-\frac{1}{3}$, $+\frac{1}{3}$, and -1 , respectively. The four contributing waves then sum up to give the simple

beat spectrum¹³

$$I(t) \propto e^{-\Gamma t/\hbar} \left| \sin\left[\frac{1}{2} \Omega_M(1,6)t\right] - \frac{1}{3} e^{-i\Delta\Omega t} \sin\left[\frac{1}{2} \Omega_M(3,4)t\right] \right|^2. \quad (2)$$

As shown in Fig. 1, $\hbar \Omega_M(1,6)$ is the magnetic splitting between the outer two transitions, $\hbar \Omega_M(3,4)$ is the magnetic splitting between the inner two transitions, and $\hbar \Delta\Omega = \Delta/2$ is the shift between the center of the (3,4) lines and the center of the (1,6) lines.

This result gives the characteristic quantum-beat pattern for any simple ⁵⁷Fe antiferromagnet. Comparing Eq. (2) with the YIG response discussed in Eq. (1) of Ref. 5, we see that the quantum-beat pattern for ⁵⁷FeBO₃ is almost the same as the fast beat modulation for YIG [for $\hat{\sigma}$ polarization with B_{int} perpendicular to $(\mathbf{k}_0, \mathbf{k}_f)$], but with $\cos[\frac{1}{2} \Omega_M(i,j)t]$ now replaced by $\sin[\frac{1}{2} \Omega_M(i,j)t]$, and a similar discussion applies. The pattern is again dominated by the leading term, $\sin^2[\frac{1}{2} \Omega_M(1,6)t]$, which arises from the interference between the strong (1,6) lines, and gives a fast beat period $2\pi/\Omega_M(1,6) = 8.1$ ns at room temperature. The contribution arising from the interference between the weak (3,4) lines, $\frac{1}{9} \sin^2[\frac{1}{2} \Omega_M(3,4)t]$, has only a small effect on the pattern but again a very perceptible modulation is caused by the interference between the (1,6) lines and the (3,4) lines. This contribution,

$$-\frac{2}{3} \cos(\Delta\Omega t) \sin\left[\frac{1}{2} \Omega_M(3,4)t\right] \sin\left[\frac{1}{2} \Omega_M(1,6)t\right],$$

alternately adds to or subtracts from the leading contribution $\sin^2[\frac{1}{2} \Omega_M(1,6)t]$ every fast beat period, again giving a "high-low" pattern to the fast beats, with the order depending on the sign of the factor $\cos(\Delta\Omega t) \times \sin[\frac{1}{2} \Omega_M(3,4)t]$. This factor changes sign at multiples of $2\pi/\Omega_M(3,4) = 51$ ns, and at odd multiples of $|\pi/2\Delta\Omega| = 114$ ns. Pronounced minima will occur whenever $\sin[\frac{1}{2} \Omega_M(1,6)t]$ and $\sin[\frac{1}{2} \Omega_M(3,4)t]$ simul-

taneously vanish, which will occur in the vicinity of multiples of $2\pi/\Omega_M(3,4) = 51$ ns. This feature is seen in Fig. 2(a). We also note that just as in the YIG case, the quantum-beat modulation of the coherent decay rate gives an initial complete suppression of coherent decay. This suppression will be characteristic of any pure nuclear reflection which is caused by a hyperfine interaction.

For our theoretical calculation of the time response, we have carried out the dynamical calculation outlined in Ref. 4, using the diagonalization procedure given in Ref. 1 to get the proper scattering amplitudes for nuclei under the influence of a crossed EFG and B_{int} . Figure 3 gives a 3D plot of the resulting time response, $|\tilde{R}(t, \delta\Theta) \hat{\sigma}|^2$, for a single reflection from ⁵⁷FeBO₃ of incident radiation of $\hat{\sigma}$ polarization. The same response is obtained for incident $\hat{\pi}$ polarization. Figure 3 shows clearly the general features discussed above: an initial suppression followed by a delayed peak response at ≈ 4 ns, followed by a sequence of rapid quantum-beat pulses of period ≈ 8 ns which damp out at a greatly enhanced decay rate $\approx (20 \text{ ns})^{-1}$. A new interesting feature is the asymmetry in the quantum-beat amplitudes above and below the Bragg angle, e.g., peaks 4, 5, and 8-12. This asymmetry gives a direct measure of the weak quadrupole interaction. In the absence of quadrupole interaction, the reflectivity has an inversion symmetry, $|R(-\delta\omega, -\delta\Theta)|^2 = |R(\delta\omega, \delta\Theta)|^2$ about the central frequency of the spectrum, above and below the Bragg angle, leading to a symmetrical time spectrum, $|R(t, -\delta\Theta)|^2 = |R(t, \delta\Theta)|^2$. Quadrupole interaction removes the inversion symmetry, giving an asymmetry in the time response,¹⁴

$$|R(t, \delta\Theta)|^2 - |R(t, -\delta\Theta)|^2 \propto -\sin(\Delta\Omega t) \sin\left[\frac{1}{2} \Omega_M(3,4)t\right] \sin\left[\frac{1}{2} \Omega_M(1,6)t\right], \quad (3)$$

which gives a direct measure of $\hbar \Delta\Omega$. Because of the proportionality to $\sin[\frac{1}{2} \Omega_M(1,6)t]$, this appears as a "Reissverschluss" (zipper) asymmetry in the amplitudes of the fast quantum beats above and below the Bragg angle. The asymmetry will be strong at times when both $\sin(\Delta\Omega t)$ and $\sin[\frac{1}{2} \Omega_M(3,4)t]$ are large, so that pronounced asymmetries occur for $t \approx 15-40$ ns (peaks 3-5) and for $t \approx 60-90$ ns (peaks 8-12), while the asymmetry will vanish for $t \approx 0-15$ ns (peaks 1 and 2) and for $t \approx 40-60$ ns (peaks 6-7). These asymmetries can be seen in the observed spectra, by comparison of Figs. 2(b) and 2(c).

For the theoretical simulation of the data, we have integrated $|\tilde{R}(t, \Theta) \hat{\sigma}|^2$ over the angular divergence of the incident beam and the mosaic spread, which we have taken to be a total Gaussian spread with $\sigma = 30 \mu\text{rad}$,

centered respectively at [Fig. 2(a)], $20 \mu\text{rad}$ below [Fig. 2(b)], and $30 \mu\text{rad}$ above the Bragg angle [Fig. 2(c)]. The agreement is generally quite good, with χ^2 values of 1.7 at, 1.5 above, and 1.9 below the Bragg angle. The fits are much better than the previous ones for YIG. We attribute this to the simpler structure of ⁵⁷FeBO₃.

In summary, we have made observations of the time response of nuclear Bragg scattering of synchrotron-radiation pulses in ⁵⁷FeBO₃. The results give a striking example of the speedup of coherent decay at the Bragg angle, and also give a quantum-beat spectrum which is characteristic for any simple ⁵⁷Fe antiferromagnet. Angular measurements of the time response were carried out, revealing an asymmetry which gives a direct measure of the weak quadrupole interaction. Dynamical cal-

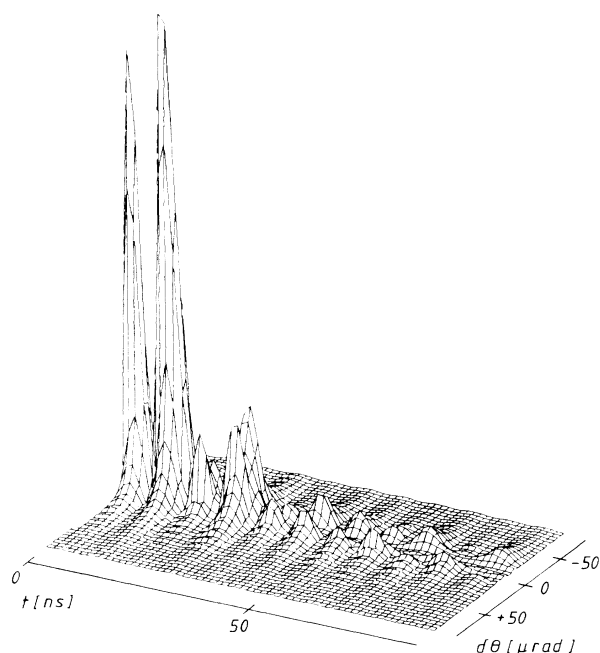


FIG. 3. 3D plot of the calculated time response $|\tilde{R}(t, \delta\Theta)\delta|^2$ following a single (111) Bragg reflection in $^{57}\text{FeBO}_3$ of incident δ -polarized radiation.

culations give excellent agreement with the observations.

This work has been funded by the Bundesministerium für Forschung und Technologie under Contracts No. 05270 GUI9 and No. KA1TUM4/7. Partial support was also provided to one of us (J.P.H.) by the Welch Foundation through Grant No. C-1049, and by the National Science Foundation through Grant No. DMR-8608248.

¹G. T. Trammell, in *Chemical Effects of Nuclear Transformations* (International Atomic Energy Agency, Vienna, 1961), Vol. I, p. 75; J. P. Hannon and G. T. Trammell, *Phys. Rev.* **186**, 306 (1969).

²A. M. Afanas'ev and Yu. Kagan, *Zh. Eksp. Teor. Fiz.* **48**, 327 (1965) [*Sov. Phys. JETP* **21**, 215 (1965)]; Yu. Kagan, A. M. Afanas'ev, and I. P. Perstnev, *Zh. Eksp. Teor. Fiz.* **54**, 1530 (1968) [*Sov. Phys. JETP* **27**, 819 (1968)].

³G. T. Trammell and J. P. Hannon, *Phys. Rev. B* **18**, 165 (1978), and **19**, 3835 (1979).

⁴E. Gerdau, R. Ruffer, R. Hollatz, and J. P. Hannon, *Phys. Rev. Lett.* **57**, 1141 (1986).

⁵R. Ruffer, E. Gerdau, R. Hollatz, and J. P. Hannon, *Phys. Rev. Lett.* **58**, 2359 (1987).

⁶U. van Bürck, G. V. Smirnov, R. L. Mössbauer, H. J. Maurus, and N. A. Semioshkina, *J. Phys. C* **13**, 4511 (1980); H. J. Maurus, U. van Bürck, G. V. Smirnov, and R. L. Mössbauer, *J. Phys. C* **17**, 1991 (1984).

⁷G. V. Smirnov and U. van Bürck, *Hyperfine Interact.* **27**, 203, 219 (1986).

⁸M. Kotrbova, S. Kadeckova, J. Novak, J. Bradler, G. V. Smirnov, and Yu. V. Shvyd'ko, *J. Cryst. Growth* **71**, 607 (1985).

⁹A. I. Chechin, N. V. Andronova, M. V. Zelepukhin, A. N. Artem'ev, and E. P. Stepanov, *Pis'ma Zh. Eksp. Teor. Fiz.* **37**, 531 (1983) [*JETP Lett.* **37**, 633 (1983)].

¹⁰G. V. Smirnov, Yu. V. Shvyd'ko, and E. Realo, *Pis'ma Zh. Eksp. Teor. Fiz.* **39**, 33 (1984) [*JETP Lett.* **39**, 41 (1984)]; G. V. Smirnov and Yu. V. Shvyd'ko, *Pisma Zh. Eksp. Teor. Fiz.* **44**, 431 (1986) [*JETP Lett.* **44**, 556 (1986)].

¹¹Yu. Kagan, A. M. Afanas'ev, and V. G. Kohn, *Phys. Lett.* **68A**, 339 (1978), and *J. Phys. C* **12**, 615 (1979).

¹²J. P. Hannon, G. T. Trammell, M. Mueller, E. Gerdau, R. Ruffer, and H. Winkler, *Phys. Rev. B* **32**, 6374 (1985).

¹³For simplicity we have dropped the higher-order modifications which take into account the ϵ shifts of the transition energies given in Fig. 1, which are unimportant for the present discussion.

¹⁴Here we have suppressed a factor $f(\delta\Theta, t)$ which vanishes as $\delta\Theta \rightarrow 0$, and which varies slowly in time relative to the other factors. A detailed discussion will be published elsewhere.